JOURNAL OF SPACECRAFT AND ROCKETS
Vol. 36, No. 3, May–June 1999

Navigation Flight Operations for Mars Pathfinder

Robin M. Vaughan,* Pieter H. Kallemeyn Jr.,* and David A. Spencer†
Jet Propulsion Laboratory, California Institute of Technology, Pasadena, California 91109
and
Robert D. Braun‡
NASA Langley Research Center, Hampton, Virginia 23665

A detailed description of the techniques used and results obtained for the interplanetary navigation of the Mars Pathfinder spacecraft is presented. Mars Pathfinder was launched on Dec. 4, 1996, and landed on Mars on July 4, 1997. To ensure a successful landing, the navigation team was required to guide the vehicle such that the flight-path-angle error was less than 1.0 deg at atmospheric entry. This relatively tight requirement was achieved through the use of a ground-based orbit determination system using Doppler and range measurements obtained from Earth stations. The resulting orbit solutions were used to design and execute four trajectory correction maneuvers needed to ensure the vehicle would make a correct atmospheric entry. More frequent orbit solutions were performed during the final two days to predict the exact time of entry and preset the onboard entry, descent, and landing sequence to deploy the parachute at the correct moment. The overall result was a successful landing less than 30 km from the intended target, well within the 100 × 200 km requirement ellipse.

Nomenclature

$\boldsymbol{B}\cdot\boldsymbol{R}$ = component of B vector orthogonal to Martian equator, km
$\boldsymbol{B}\cdot\boldsymbol{T}$ = component of B vector parallel to Martian equator, km
γ = atmospheric entry flight-path angle, deg
ΔV = velocity change, m/s
θ = orientation of B-plane uncertainty ellipse, deg

I. Introduction

MARS Pathfinder, part of NASA's Discovery Program of low-cost missions for planetary exploration, was designed to demonstrate a low-cost, reliable system for entering the Martian atmosphere and placing a lander safely on the surface. Mars Pathfinder carried a science payload that returned data on the atmosphere, meteorology, geology and morphology, and the elemental composition of rocks and soil near the lander. A key element of this payload was the Sojourner microrover, which was the first mobile vehicle ever operated on the surface of another planet.

The spacecraft traveled along the transfer trajectory from Earth to Mars shown in Fig. 1. During the seven-month journey between planets, the lander and its science payload were enclosed in an aeroshell (backshell and heatshield) that was attached to a cruise stage as shown in Fig. 2. The cruise stage contained the propulsion unit, star and sun sensors, solar arrays, and other subsystems needed to travel from Earth to Mars. The lander contained the flight computer, X-band telecommunication system, and all engineering systems that were used during surface operations. Telecommunications and navigation tracking during cruise were performed using the medium-gain antenna on the cruise stage and, primarily, the 34-m-diam high-efficiency antennas at the three sites of NASA's Deep Space Network (DSN). Prime navigation tracking data types were coherent, two-way (X-band) Doppler and ranging.

Four trajectory correction maneuvers (TCMs) were planned and executed during cruise. The navigation system was required to perform these maneuvers using less than 105 m/s over the course of the mission. Because the Pathfinder spacecraft made a direct entry into the Martian atmosphere from its interplanetary trajectory, the navigation system was required to control the flight-path angle at entry. This angle had to remain within 1.0 deg of the nominal value of −14.2 deg to ensure a safe descent. The final navigation requirement was to land within a 100 × 200 km elliptical footprint surrounding the selected target landing location of 326.9°E longitude and 19.244°N latitude.[1,2]

This paper documents the actual navigation performance for the mission in three main sections. First, the process of estimating the spacecraft trajectory from the radiometric tracking data [known as orbit determination (OD)] is summarized in Sec. II. The OD subtopics addressed are force modeling, Doppler and range data quality, and the OD filter configuration. Section II ends with a summary of the OD solutions used for the design of each TCM. Section III discusses the maneuver design process. Subtopics in this section are targeting requirements, maneuver execution modes, and a comparison of the actual performance of each TCM with its designed value. Section IV describes the OD activities performed in the final 48 h in support of the entry, descent, and landing (EDL) phase, including a summary of the key OD solutions performed during this time.

II. Orbit Determination

Spacecraft Force Modeling

Accurate modeling of all forces acting on the spacecraft was necessary to properly predict the orbit solutions forward to Mars encounter. The double-precision trajectory (DPTRAJ) software set, developed at the Jet Propulsion Laboratory (JPL), was used to integrate these models and to produce trajectories for use in mission operations. The largest forces acting on the Pathfinder spacecraft were the gravitational attraction of the sun and planets. The only other known forces acting during cruise were solar radiation pressure and thrusting events for attitude control and TCMs. All attitude control turns and spin rate changes were modeled as instantaneous velocity changes with magnitudes ranging from 0.5 to 7 mm/s. A total of 24 such events were eventually included in the filter runs. The four TCMs were modeled as a set of either finite or instantaneous burns, depending on their magnitude and execution mode.[3]

Solar radiation pressure (SRP) contributed a small, but significant, continuous force on the spacecraft. DPTRAJ performs SRP modeling by a series of basic components (flat plates, cylinders, and spheres) that represent the size and reflective properties of illuminated components of the spacecraft. A flat plate was used to represent the solar array disk of the cruise stage, the dominant component of the Mars Pathfinder SRP model. The launch vehicle adapter and the

Received Jan. 25, 1998; revision received Aug. 15, 1998; accepted for publication Feb. 22, 1999.

*Senior Staff Engineer, Navigation and Flight Mechanics Section. Member AIAA.
†Mission Manager, Mars Surveyor '01 Project. Member AIAA.
‡Senior Aerospace Engineer, Space Systems and Concepts Division. Senior Member AIAA.

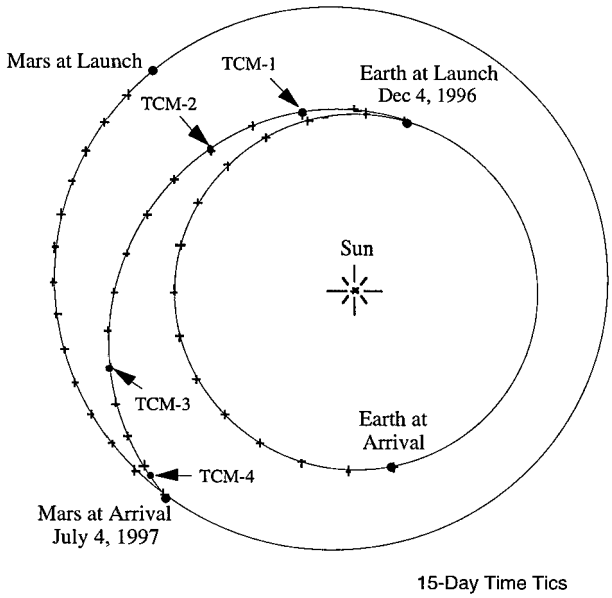

Fig. 1 Mars Pathfinder interplanetary trajectory.

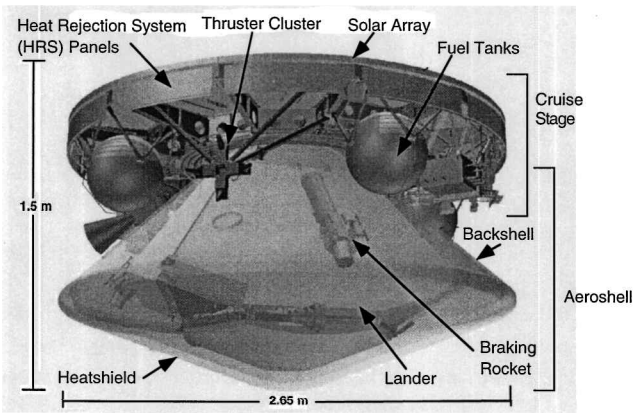

Fig. 2 Mars Pathfinder flight system.

heat rejection system (HRS) panels, also on the cruise stage, were represented by a flat plate and cylinder, respectively. Accurately modeling the effect of the backshell, however, proved challenging because the backshell had a nonstandard shape and was variably shaded by the cruise stage during the flight. During the seven months of cruise, different SRP models of backshell were used and evaluated. The initial SRP model used a simple flat plate to represent the backshell active for the entire cruise. The second model also represented the backshell as a flat plate, but only after March 1997, because prior to then the majority of the backshell was shaded and, therefore, would not have contributed significantly to the overall SRP effect. A third attempt tried two separate components for the backshell: a cylinder active before April 1997 and a flat plate active thereafter. The fourth and final model returned to using a flat plate for the entire cruise, but with modified area and reflective properties. Each of these SRP models were attempts to account for the changing solar illumination on the backshell; the orientation of the backshell component relative to the cruise stage components, as well as its activation time, was based on the history of the solar aspect angle over the mission.[3]

The navigation team experimented with the set of parameters estimated for each component along with the number, type, and active periods for components in the solar pressure model. After uncovering some inconsistencies in filter results when switching component sets during a data arc and estimating multiple parameters for each component, it was decided to estimate only area scale factors for each component and to model the backshell as a flat plate over the entire cruise. This was the strategy employed for all OD operations solutions following TCM 4.

Small modeling errors and potential unknown forces such as outgassing were accommodated in the filter by including a set of stochastic nongravitational accelerations. These parameters were tightly constrained by the choice of a priori sigmas so that they were not confused with known forces already in the filter model.

Doppler Data Quality

The circular polarization of the radio signals and a slight offset of the spacecraft's antenna boresight from the spin axis caused both a bias and a sinusoidal modulation to appear in the Doppler data. The amplitude of the sinusoidal modulation increased with increasing angle between the spacecraft's spin axis and the line of sight to Earth. Figure 3 shows the final postfit Doppler residuals over the entire cruise period from launch to entry (December 1996–July 1997). Residuals represent the difference between the actual measurement values and predicted values from the OD filter solution. The sinusoidal modulation is clearly seen in the passes before TCM 1, when the spin axis was pointed toward the sun, at high angles from the Earth. The scatter for these passes is large, ranging from 0.01 to 0.03 Hz (0.18 to 0.53 mm/s). Early OD solutions treated this signature as simply an increase in data noise, and the data were consequently deweighted. Typical Doppler weights for the period before TCM 1 ranged between 0.025 and 0.10 Hz (0.44 and 1.8 mm/s), assuming a 60-s count time. The Doppler passes in Fig. 3 after TCM 1 appear much more compact, when the spacecraft was reoriented to an Earth-pointed attitude. The scatter of points within each pass decreased to 0.00173 Hz (0.031 mm/s) between TCMs 1 and 2. The Doppler noise level continued to decrease, averaging 0.0010 Hz (0.018 mm/s) per pass between TCMs 2 and 3 and 0.0014 Hz (0.025 mm/s) per pass after TCM 3. These later Doppler data were ultimately weighted at 0.006 Hz (0.11 mm/s), for a 60-s count time.

The bias component of the Doppler spin signature was preapplied to the data before filtering and so is not visible in Fig. 3. This bias is a function of the spacecraft spin rate. The final, critical OD solutions supporting EDL preparations used a special Doppler bias model derived from the actual history of spin rate values taken from spacecraft telemetry.

Ranging Data Quality

The DSN uses the sequential ranging assembly (SRA) to calculate the round-trip delay from station to spacecraft and back. Measurements from the SRA are provided in range units (RU), with 7 RU equaling 1 m. Prelaunch requirements levied on the ranging system imposed a 1σ noise (or jitter) level no greater than 1.0 m (7 RU) within each pass. However, the range noise persisted at higher levels until late May 1997, as seen in Fig. 4, which plots the postfit ranging residuals for the entire cruise. The first data returned after launch exhibited 1σ noise between 13 and 27 RU (1.86–3.8 m). As with the Doppler, the range noise decreased after TCM 1 when the spacecraft was oriented to an Earth-pointed attitude. The DSN ranging system uses the Doppler signal to assist in forming the ranging measurements, and the spin signature imposed on the Doppler evidently degraded the early ranging measurements. Although the noise level had improved after TCM 1, it remained slightly above the desired value, varying between 7.4 and 11.7 RU (1.06–1.67 m), until March 1997. The spacecraft's ranging system configuration was changed at this time, significantly lowering the 1σ range noise level for passes from Deep Space Station (DSS) 45 (Canberra, Australia) and DSS 65 (Madrid, Spain) to 2.23 RU (0.32 m). But the passes from DSS 15 (Goldstone, California) remained at an unexpectedly higher noise level, eventually increasing to about 23.3 RU (3.3 m) by the end of May 1997. A concentrated effort by DSN personnel eventually traced this problem to a faulty hardware component at the station. This component was replaced by May 30, 1997, and subsequent ranging passes from DSS 15 had noise levels comparable to the other two DSN sites. The last 35 days of ranging data before Mars arrival had an average 1σ per-pass noise of 4.0 RU (0.57 m), well within the required level.

The range data weight in OD solutions was varied throughout the data arc to account for the changing noise level. Data before March 7, 1997, were typically weighed at 21 RU (3 m). DSS 15 range data continued to be weighed at this larger value up to May

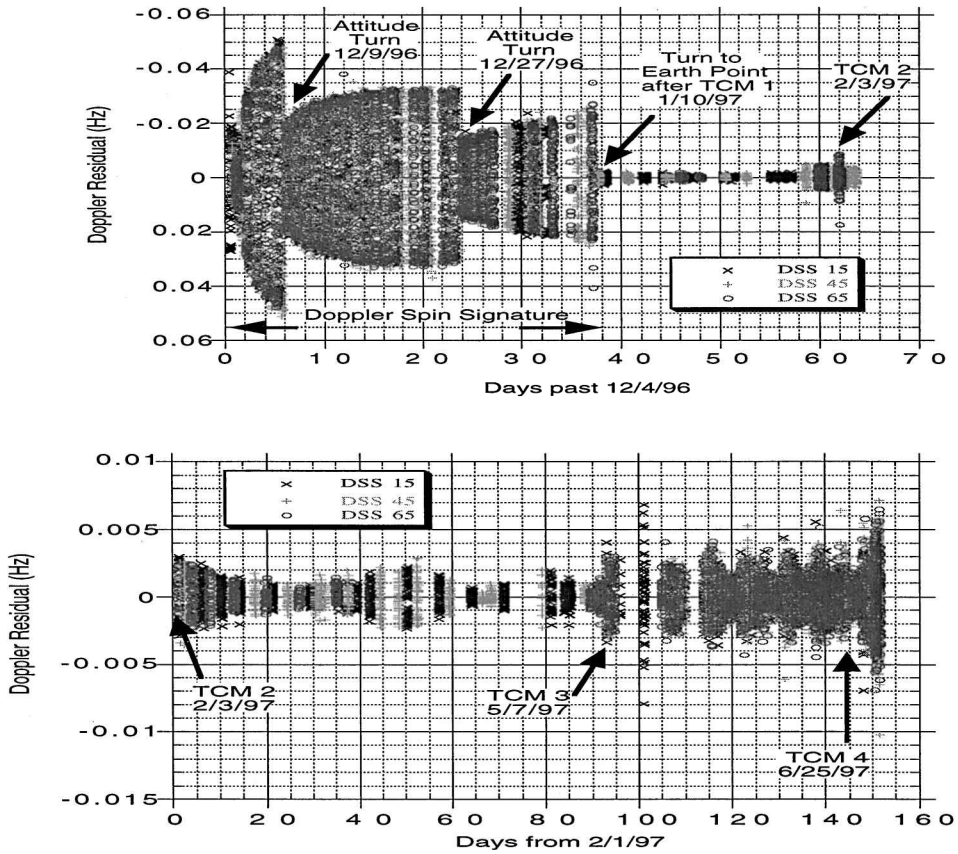

Fig. 3 Postfit Doppler residuals from launch to Mars arrival.

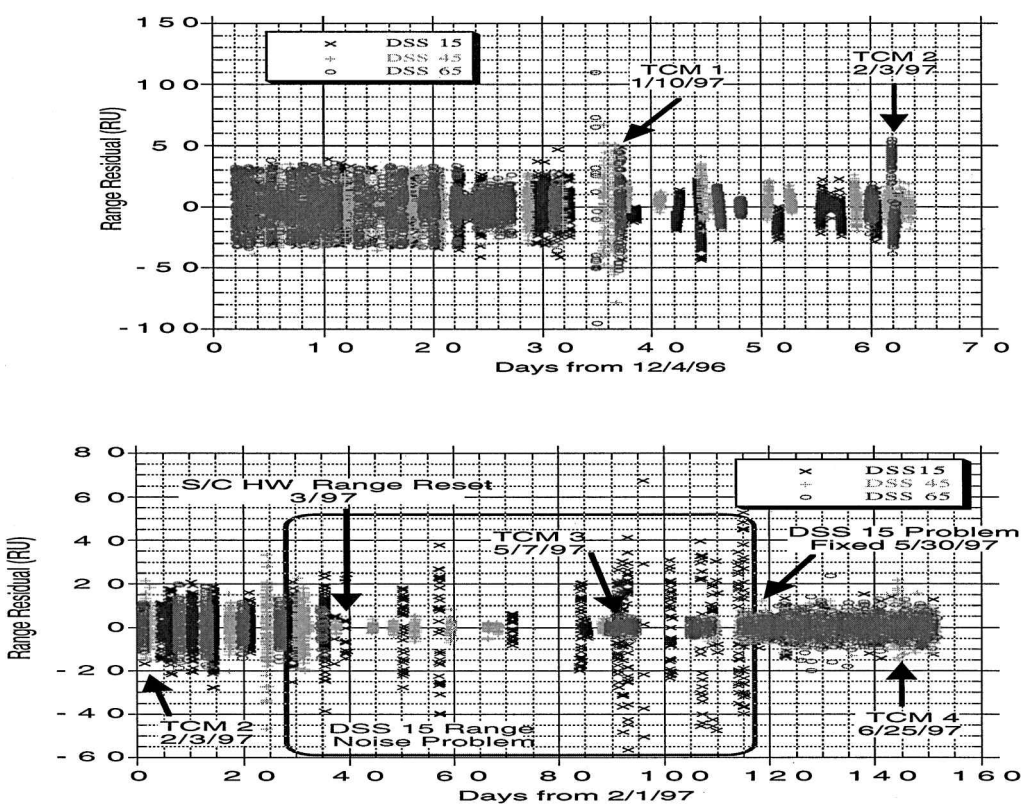

Fig. 4 Postfit range residuals from launch to Mars arrival.

Table 1 *B*-plane state, TCA, and 1σ uncertainties

OD solution	Data arc	$\boldsymbol{B}\cdot\boldsymbol{R}$, km	$\boldsymbol{B}\cdot\boldsymbol{T}$, km	TCA, universal time constant (UTC)	1σ SMA axis, km	1σ SMI axis, km	θ, deg	1σ TCA, s
TCM 1	12/9/1996–1/2/1997 (24 days)	279,321.23	386,696.07	7/3/1997 09:14:57	100.64	11.066	24.44	25.93
TCM 2	12/4/1996–1/26/1997 (53 days)	8,491.72	9,767.62	7/4/1997 15:45:26	249.03	243.915	31.54	80.02
TCM 3	2/4/1997–4/29/1997 (84 days)	−1,790.15	−4,494.02	7/4/1997 16:52:52	34.49	30.717	106.99	6.21
TCM 4	2/4/1997–6/23/1997 (139 days)	−1,852.63	−4,250.28	7/4/1997 16:54:21	17.44	4.192	109.59	0.38

Table 2 *B*-plane and TCA targets for TCMs 1–4

Maneuver	Date	Target $\boldsymbol{B}\cdot\boldsymbol{R}$, km	Target $\boldsymbol{B}\cdot\boldsymbol{T}$, km	Target TCA (UTC on 7/4/1997)
TCM 1	Launch + 37 days (1/10/1997)	−1856.93	−4263.91	16:53:43.20
TCM 2	Launch + 61 days (2/3/1997)	−2004.00	−4554.00	16:53:43.26
TCM 3	Mars − 58 days (5/7/1997)	−1855.60	−4264.16	16:54:22.128
TCM 4	Mars − 9 days (6/25/1997)	−1855.60	−4264.16	16:54:22.128

30, 1997, whereas DSS 45 and 65 data were weighed more tightly at just 4 RU (0.57 m). After May 30, 1997, data from all sites were weighed at 4 RU.

Ranging biases of various types were routinely employed as part of the OD filtering strategy, resulting in the zero-mean behavior of the residuals seen in Fig. 4. These included a constant bias for all ranging data and stochastic biases whose values varied for each pass. Prelaunch expected values for the pass-dependent biases were on the order of 10 RU. In-flight OD solutions consistently yielded values from 20 to 50 RU for these biases. The a priori sigma for these parameters in the OD filter was increased to 40 RU to reflect these larger values. Fixed biases for all passes from a specific DSS site also had to be employed to account for three periods of observed biases in the ranging data. Appropriate values for the two earliest of these were obtained and preapplied to the affected data prior to the final week before landing. A final site-dependent bias between the DSS 65 ranging passes and the 15 and 45 passes was unresolved before landing. The a priori sigma on the DSS 15 and 45 bias parameters was set at 7 RU; whereas the DSS 65 parameter's sigma was set at 30 RU. The estimated value of the DSS 65 bias in these runs ranged from −15 to −20 RU relative to the DSS 15 and 45 passes.[3]

Orbit Determination Filter Configuration

Orbit determination for Mars Pathfinder was performed with the Orbit Determination Program developed at JPL and used for nearly all interplanetary flight projects. It uses a linearized batch-sequential filter on a variety of data to update a user-specified set of parameters describing the flight path and/or data. Prior to Mars Pathfinder, OD filters for deep space navigation have been configured to estimate a mix of (constant) bias, stochastic, and considered parameters. The set of bias parameters typically includes the known nongravitational forces acting on the spacecraft. Pathfinder's OD solutions followed this pattern, estimating solar pressure, velocity changes from TCMs and attitude control events, and the spacecraft epoch state as bias parameters. DSN station locations were also estimated as bias parameters as were Earth and Mars ephemeris parameters in runs performed within 10 days of landing. A constant range bias for spacecraft hardware delay, constant range biases for each of the DSN sites, and a constant Doppler bias were also added.

Considered parameters are parameters whose statistics influence the overall statistics of the OD solution but do not affect the estimated parameter values. In a departure from the traditional approach, no considered parameters were employed in the Pathfinder filter. Instead, new stochastic parameters were introduced to model data error sources that were formerly treated as considered parameters. An important group of these new stochastic parameters were the pass-dependent biases for the range and Doppler data. The introduction of these biases for the range data is called the precision range technique and allowed the data to be weighted at its inherent accuracy of a few meters. Pass-dependent Doppler biases were included to account for small deviations from the nominal spin rate. Troposphere and ionosphere transmission effects on the radio signal, Earth rotation, and

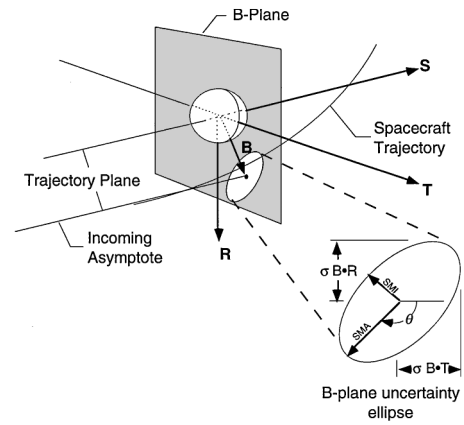

Fig. 5 *B*-plane definition.

polar motion parameters were also treated as stochastic parameters. The remaining stochastic parameters were components of accelerations acting in the radial and transverse directions. One or all of these components were included to account for small, unknown errors in the force model. The success of Pathfinder navigation has provided valuable in-flight validation of this enhanced filter configuration, with its associated precision ranging technique.[1,2,4,5]

OD Results for TCM Design

The results of the OD solutions leading to the design of TCMs 1–4 are summarized in Table 1. Predicted spacecraft state at Mars arrival is given as coordinates in a Mars-centered *B*-plane coordinate system shown in Fig. 5. The *B* plane is perpendicular to the incoming asymptote of the spacecraft's trajectory (called the ***S*** direction) and contains the two axes ***R*** and ***T***. ***T*** is defined as the intersection of the *B* plane with the Mars mean equator of date. Predicted position in the *B* plane is given in Table 1 as a pair of ***R*** and ***T*** coordinates ($\boldsymbol{B}\cdot\boldsymbol{R}$ and $\boldsymbol{B}\cdot\boldsymbol{T}$) for the location where the asymptote intersects the *B* plane. Uncertainty in *B*-plane position is represented by the size and orientation of a 1σ error ellipse around the predicted position. The sizes of these ellipses are given as semimajor (SMA) and semiminor (SMI) axes lengths, whereas the ellipse orientation is given by the angle to the SMA axis direction measured clockwise from the ***T*** axis (θ). Predicted position in the ***S*** direction is given in Table 1 by the time of closest approach (TCA), or time of periapsis, and its associated 1σ uncertainty. Because Mars Pathfinder landed before its approach orbit's periapsis was reached, this TCA parameter did not reflect any real mission event, but was instead used to compare solutions against each other.

III. Maneuver Design

Targeting and Design of TCMs 1–4

The target trajectory conditions for TCMs 1–4 are presented in Table 2 as $\boldsymbol{B}\cdot\boldsymbol{R}$ and $\boldsymbol{B}\cdot\boldsymbol{T}$ coordinates in the Mars-centered *B*-plane

coordinate system and an associated TCA to Mars. These quantities are chosen for ease of comparison with the OD solution results given in Table 1. The targets for TCMs 3 and 4 were based solely on the required entry and landing conditions. The targets for TCMs 1 and 2, however, could have been biased from this aimpoint to satisfy a mission requirement dictating a less than $1.0E-4$ probability of the vehicle impacting the Martian surface at 1000 ft/s or more (for planetary contamination reasons). Analysis of the actual injection accuracy and OD knowledge at the time of TCM 1 design showed that this requirement would be satisfied without adding any bias to the direct entry target point. Therefore, the target aimpoint for TCM 1 listed in Table 2 is very close to that of TCMs 3 and 4. Subsequent OD solutions reflecting TCM 1 execution showed that a bias would have to be added to satisfy the surface impact speed constraint at the time of TCM 2 design, so that its target parameters differ significantly from those of the other three maneuvers.

Targeting for TCMs 1, 3, and 4 was based on achieving the required flight-path angle at a specified radial distance of 3522.2 km from the center of Mars and subsequently landing within a 100×200 km ellipse in Ares Vallis. OD solutions provided the predicted arrival geometry and time of the Mars atmospheric entry. The descent trajectory through the atmosphere then determined the landing site associated with this arrival point. Aerodynamic modeling programs were used to compute the trajectory dynamics during descent and to target to the desired landing site.[6] Standard navigation software was used to target the interplanetary trajectory to the required atmospheric interface geometry. The B-plane coordinates and arrival time associated with the desired descent and landing conditions were obtained through iterative application of these programs.[3,6] The navigation software was also used to calculate the required velocity change ΔV vector for each maneuver. The current best estimate of the orbit, the nominal time of the TCM and the target encounter conditions were used together to calculate the required ΔV for the upcoming TCM. The times and overall design ΔV vectors for each TCM are listed in Table 3, expressed in the Earth Mean Equator and Equinox of Epoch J2000 (EME2000) coordinate France. The maneuver design calculations assumed an instantaneous application of the total ΔV for TCMs 3 and 4 but assumed a finite burn duration for the larger TCMs 1 and 2.

Maneuver Execution Modes

The Pathfinder propulsion system had two clusters of four thrusters: collectively these eight thrusters could produce either axial thrusts, which were aligned with the spin axis of the spacecraft, or lateral thrusts roughly perpendicular to the spin axis. Depending on the spacecraft's attitude relative to the direction of the desired ΔV vector, subsets of the thrusters could be fired to add vectorially to the total ΔV (Refs. 2 and 7). TCM 1 was implemented using only a single session of axial thrusting. A single axial thrust could also have been done for TCM 2, but both lateral and axial thrusting would be necessary for TCMs 3 and 4 given the preferred spacecraft attitude for late cruise. Lateral and axial thrusting would also be required for a potential TCM 5 that was added as a contingency activity to be performed within the last 24 h before entry. Because these TCMs were critical for Mars atmospheric entry targeting, it was decided to test lateral thrusting performance at TCM 2 and again at TCM 3. TCM 2 was performed as one axial followed by one lateral thrusting session. TCM 3 was performed in three segments: a lateral, an axial, and another lateral session. No problems were encountered with the lateral thrusting portions added to TCMs 2 and 3, verifying the design approaches for TCMs 4 and 5. TCM 4 was executed with a single lateral segment followed by an axial segment. Although the required ΔV turned out to be very small, it was decided to perform TCM 4 maneuver to minimize the probability of having to do TCM 5. The performance of all four TCMs were so accurate that TCM 5 was not required.

Maneuver Performance

The actual ΔV provided by the spacecraft's propulsion system were estimated as part of the on-going orbit determination process using tracking data obtained during and after each TCM. Table 4 shows the best estimates of the actual ΔV vectors for TCMs 1–4. A comparison of the estimates with the design values (Table 3) reveals that maneuver execution was quite accurate for Mars Pathfinder. The magnitude errors achieved in flight ranged from 0.2 to 4%. Pointing errors, computed as the angle between the design direction and the best estimated direction for the TCMs, were typically less than 0.15 deg, with a slightly larger value of just over 0.5 deg for the second lateral segment of TCM 3. Both of these types of errors were well within the performance requirements levied on the spacecraft's propulsion system. The total actual ΔV used for Mars Pathfinder's TCMs was 32.733 m/s, well within the propulsion system's total capability of 105 m/s.

IV. Navigation Support for EDL

Prelaunch analyses had shown that no significant improvement in OD knowledge would occur after TCM 4 execution until the last 48 h before entry when the Mars gravitational signature would begin to be sensed in the Doppler data at levels greater than typical Doppler noise. Trajectory uncertainties would decrease from this time, with the largest decrease occurring in the final 24 h. This improved trajectory knowledge was put to several important uses. First, it was used to update key parameters in the flight software controlling the mechanisms and events for a safe descent and

Table 3 Design values for TCMs 1–4

Maneuver	Design execution time, UTC	Design ΔV vector[a] in EME2000 (inertial) coordinates X, m/s	Y, m/s	Z, m/s	Magnitude, m/s
TCM 1	1/10/1997 02:00	17.301	−25.321	5.899	31.229
TCM 2	2/3/1997 23:00	1.1193	−1.1231	0.0352	1.5860
TCM 3	5/7/1997 01:00	0.0762	0.0630	0.0362	0.1053
TCM 4	6/25/1997 17:00	0.0105	−0.0138	−0.0068	0.0186

[a]Ideal ΔV determined to achieve the target conditions.

Table 4 Estimated values for TCMs 1–4

Maneuver	Design execution time, UTC	Estimated ΔV vector[a] in EME2000 (inertial) coordinates X, m/s	Y, m/s	Z, m/s	Magnitude, m/s
TCM 1	1/10/1997 02:00	16.6367	−24.4114	5.6403	30.077
TCM 2	2/3/1997 23:00	1.1223	−1.1340	0.0365	1.5959
TCM 3	5/7/1997 01:00	0.0764	0.0725	0.0382	0.1120
TCM 4	6/25/1997 17:00	0.0105	−0.1374	−0.0068	0.0186

[a]Actual performance of the TCM as determined from subsequent OD.

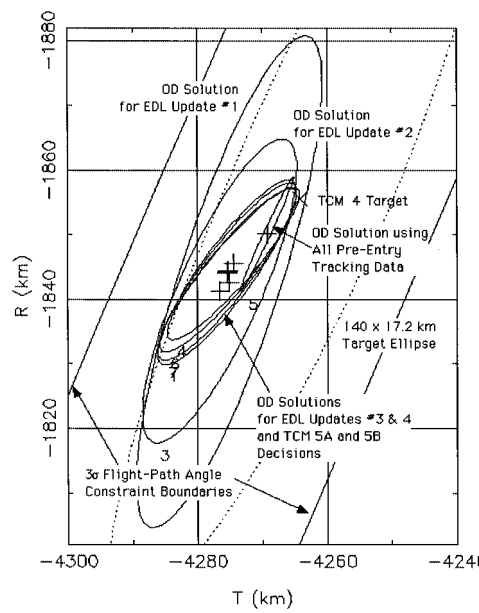

Fig. 6 EDL OD solutions 1σ B-plane error ellipses.

initial surface deployment. Second, the predictions at the DSN station were updated with the new trajectory profile to increase the chances of remaining in contact with the spacecraft for as long as possible during descent. Finally, two opportunities were inserted to correct any unexpected trajectory deviations by performing a fifth maneuver, TCM 5. Four opportunities to update the EDL parameters were planned at 37, 22, 9, and 4 h before entry. Two windows were identified for possible TCM 5 execution, one at 10.5 h (TCM 5A) and the other at 5.5 h before entry (TCM 5B). A single time was chosen for the DSN predictions update at 2.5 h before entry. The navigation team worked around the clock to provide new OD solutions to update the trajectory and landing site knowledge at each of these events.[7]

Numerical results from the actual OD solutions performed during the final 48 h of flight are presented in Tables 5–7. Table 5 gives the predicted B-plane positions and TCAs and Table 6 their associated uncertainties, as was done in Table 1. Because of the importance of entry flight-path angle γ, predictions and uncertainties for it are also given in Tables 5 and 6. For a lander mission like Pathfinder, the navigation uncertainty can be expressed in terms of an ellipse on the surface, or footprint, centered around the predicted landing site. Centers and sizes for the footprints corresponding to the B-plane error ellipses are given in Table 7. A graphical history of these OD solutions is shown in the B plane in Fig. 6 and on the surface in Fig. 7. Figures 6 and 7 clearly show the consistency of the OD results obtained at each of the EDL decision points.

The navigation team continued to generate OD solutions as new tracking data were received, right up to the last minutes before entry. The final best estimate from pre-entry tracking data used two-way coherent Doppler data taken up to 1.3 h before entry and range data collected up to 3.4 h before entry. This case is labeled "All data" in Tables 5–7. The size of the landing footprint had diminished considerably with incorporation of the later data, as shown in Figs. 7 and 8 (the ellipse labeled "OD solution using all pre-entry tracking data"). The new landing footprint was only 15×8 km, assuming no dispersions due to atmosphere or vehicle aerodynamic mismodeling. This assumption was acceptable for earlier OD solutions where entry state uncertainties dominated the footprint size. As knowledge of the entry state improved, the relative significance of the atmospheric and aerodynamic dispersions increased. Figure 8 shows the 15×8 km all-data ellipse compared with a slightly larger ellipse representing the results of a Monte Carlo analysis of the entry trajectory that incorporated appropriate uncertainties in aerodynamic and atmospheric conditions. This result is represented numerically in Table 7 as the case labeled "All data + descent dispersions."

Independent estimates of Pathfinder's landing location have been computed using data taken after surface deployment. The first of these is derived by triangulation from surface features identified in images taken by the lander's camera.[8] The second estimate is derived by processing Doppler and range measurements from Pathfinder during the surface phase of the mission, between July and September 1997, along with similar data from the Viking landers.[9] These two estimates of landing site location are labeled "Image triangulation" and "Surface tracking data" in Table 7 and are shown graphically in Fig. 8. These solutions are reasonably consistent with the final navigation results, especially when descent dispersions are included

Table 6 EDL OD solution associated uncertainties

	1σ Uncertainty ellipse				
Solution	SMA, km	SMI, km	θ, deg	σ_{TCA}, s	σ_γ, deg
EDL update 1	13.303	2.615	108.016	0.227	0.146
EDL update 2	8.542	2.127	114.077	0.158	0.104
TCM 5A	5.816	1.357	126.059	0.115	0.090
EDL update 3	5.674	1.254	127.266	0.113	0.089
TCM 5B	5.380	1.117	129.268	0.108	0.089
EDL update 4	5.106	1.052	130.576	0.103	0.089
All data	3.246	0.176	114.972	0.023	0.001

Table 5 EDL OD solution B-plane state, TCA, and entry flight-path angle γ

Solutions	Data cutoff, UTC	$\boldsymbol{B} \cdot \boldsymbol{R}$, km	$\boldsymbol{B} \cdot \boldsymbol{T}$, km	TCA, UTC on 7/4/1997	γ, deg
EDL update 1	7/2/1997 19:46	−1842.67	−4275.09	16:54:22.6	−13.942
EDL update 2	7/3/1997 18:48	−1841.28	−4276.58	16:54:22.6	−13.902
TCM 5A	7/4/1997 02:54	−1844.19	−4275.45	16:54:22.6	−13.896
EDL update 3	7/4/1997 04:46	−1844.27	−4275.43	16:54:22.594	−13.896
TCM 5B	7/4/1997 07:46	−1844.52	−4275.27	16:54:22.589	−13.898
EDL update 4	7/4/1997 10:46	−1844.58	−4274.46	16:54:22.516	−13.914
All data	7/4/1997 15:41	−1850.17	−4269.23	16:54:22.386	−14.061

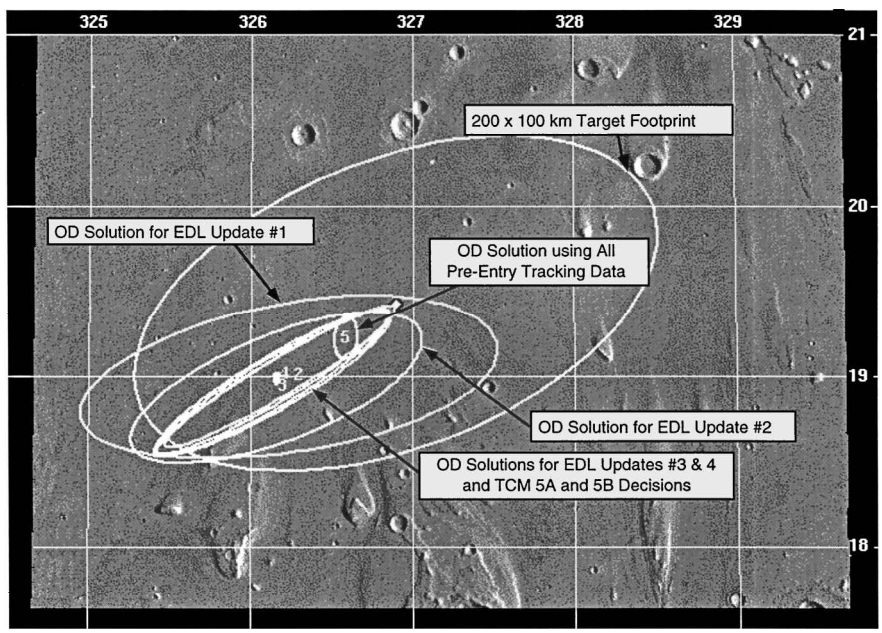

Fig. 7 Predicted surface footprints (3σ) for EDL OD solutions.

Table 7 EDL OD solution landing site and 3σ surface footprints

Solution	Longitude, °E	Latitude, °N[a]	Downtrack 3σ, km	Crosstrack 3σ, km	Orientation, deg[b]
Target	326.9	19.244	N/A	N/A	N/A
EDL update 1	326.2294	18.8238	154.209	51.784	8.21
EDL update 2	326.1944	18.7629	112.565	37.400	20.586
TCM 5A	326.1634	18.7924	98.301	18.606	29.460
EDL update 3	326.1617	18.7929	97.759	16.931	29.896
TCM 5B	326.1671	18.7985	97.600	12.988	30.423
EDL update 4	326.2063	18.8291	96.607	12.988	29.836
All data	326.5875	19.0438	15.116	8.395	84.457
All data + descent dispersions	326.48	19.004	41.458	14.807	18.631
Image triangulation	326.45	19.14	N/A	N/A	N/A
Surface tracking data	326.4762	19.095	N/A	N/A	N/A

[a]Measured as areocentric. [b]Measured counterclockwise from east.

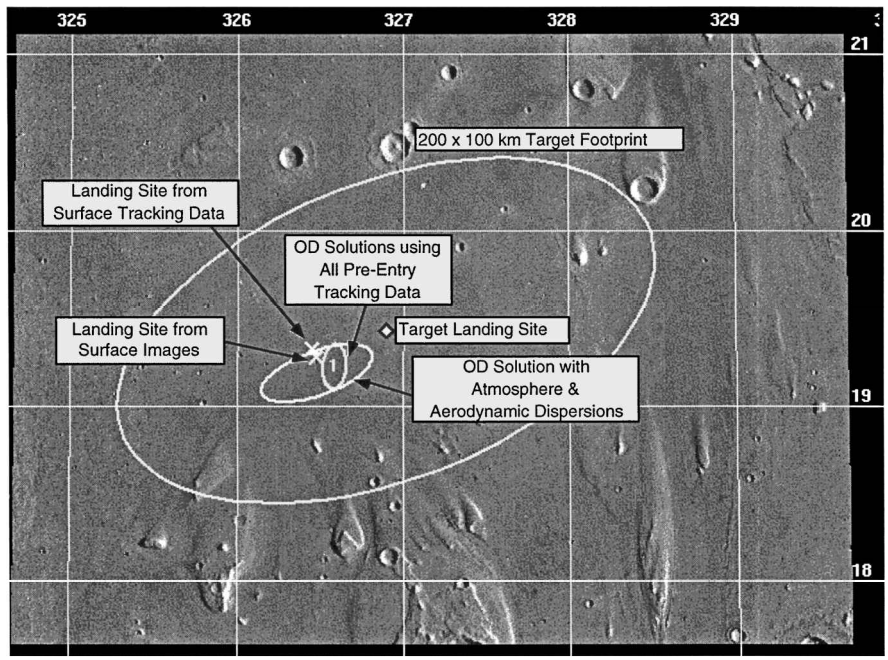

Fig. 8 Best estimates of Pathfinder's landing site.

in the estimate. All solutions give points roughly southwest of and less than 30 km from the target landing site.

V. Conclusions

All of the requirements placed on Mars Pathfinder navigation were met with ample margins. The lander came to rest within 30 km of the target location, well within the goal of a 200 × 100 km footprint around the target. The final estimated flight-path angle at entry was −14.06 deg, just 0.14 deg off from the nominal value of −14.2 deg and well within the required 1.0-deg dispersion from the nominal. The total ΔV used for trajectory corrections was 32.7 m/s, well under the propulsion system's 105-m/s limit.

One of the major accomplishments of Mars Pathfinder navigation was the successful implementation of the enhanced filter configuration and the precision ranging technique for spacecraft orbit determination. These methods allowed the necessary OD accuracy to be achieved using only Doppler and ranging without the addition of other data types such as optical images or ΔVery Long Baseline Interferometry. Pathfinder has validated the use of this filter configuration for actual flight operations. These techniques will be employed in navigating future Mars missions.

Another significant accomplishment was the integration of existing navigation software for modeling an interplanetary trajectory with software modeling the descent trajectory once in the atmosphere. Coordinated use of these programs was necessary to target the late cruise maneuvers for a landing at the desired surface location. This enhanced software tool set also allowed optimization of the spacecraft's descent conditions based on rapid and frequent OD updates using the latest available tracking data in the final hours before entry.

Acknowledgments

The work described in this paper was performed at the Jet Propulsion Laboratory, California Institute of Technology, under contract with NASA. The navigation team would like to express its gratitude to the entire Mars Pathfinder flight team for their support, hard work, and dedication throughout the mission.

References

[1]Kallemeyn, P. H., "Mars Pathfinder Navigation Plan," Jet Propulsion Lab., JPL Document D-11349, PF-220-NP, California Inst. of Technology, Pasadena, CA, July 1994.

[2]Kallemeyn, P., Spencer, D. A., Vaughan, R., and Helfrich, C., "The Mars Pathfinder Navigation System," AIAA Paper 96-3656, July 1996.

[3]Kallemeyn, P., Vaughan, R., Spencer, D., and Braun, R., "Mars Pathfinder Navigation Report," Jet Propulsion Lab., JPL IOM 312.A/98-030, California Inst. of Technology, Pasadena, CA, Jan. 1998.

[4]Estefan, J. A., Pollmeier, V. M., and Thurman, S. W., "Precision X-Band Doppler and Ranging Navigation for Current and Future Mars Exploration Missions," American Astronautical Society, AAS Paper 93-250, Aug. 1993.

[5]Thurman, S. W., and Pollmeier, V. M., "Guidance and Navigation for the Mars Pathfinder Mission," *Acta Astronautica*, Vol. 35, Suppl., 1995, pp. 545–554.

[6]Spencer, D. A., and Braun, R. D., "Mars Pathfinder Atmospheric Entry: Trajectory Design and Dispersion Analysis," *Journal of Spacecraft and Rockets*, Vol. 33, No. 5, 1996, pp. 670–676.

[7]Braun, R. D., Spencer, D. A., Kallemeyn, P. H., and Vaughan, R. M., "Mars Pathfinder Atmospheric Entry Navigation Operations," *Journal of Spacecraft and Rockets*, Vol. 36, No. 3, 1999, pp. 348–356.

[8]Golombek, M. P., Cook, R. A., Economou, T., Folkner, W. M., Heldemann, A. F. C., Kallemeyn, P. H., Knudsen, J. M., Manning, R. M., Moore, H. J., Parker, T. J., Reider, R., Schofield, J. T., Smith, P. H., and Vaughan, R. M., "Overview of the Mars Pathfinder Mission and Assessment of Landing Site Predictions," *Science*, Vol. 278, No. 5344, 1997, pp. 1743–1748.

[9]Folkner, W. M., Yoder, C. F., Yuan, D. N., Standish, E. M., and Preston, R. A., "Interior Structure and Seasonal Mass Redistribution of Mars from Radio Tracking of Mars Pathfinder," *Science*, Vol. 278, No. 5344, 1997, pp. 1749–1752.

R. D. Braun
Guest Editor